Throughput Requirements for RAN Functional Splits in 3D Networks

MohammadAmin Vakilifard, Tim Düe, Mohammad Rihan, Maik Röper,
Dirk Wübben, Carsten Bockelmann, Armin Dekorsy
Department of Communications Engineering, *University of Bremen*, Bremen, Germany.
{vakilifard, duee, elmeligy, roeper, wuebben, bockelmann, dekorsy}@ant.uni-bremen.de

***Abstract*—The rapid growth of non-terrestrial communication necessitates its integration with existing Terrestrial Network (TN), as highlighted in 3GPP Releases 16 and 17. To manage this complex structure effectively, the adoption of a Radio Access Network (RAN) architecture with Functional Split (FS) offers advantages in flexibility, scalability, and cost-efficiency. RAN achieves this by disaggregation of functionalities into three separate units. Analogous to the TN approach, 3GPP is extending this concept to non-terrestrial platforms as well. This work presents a general analysis of the requested Fronthaul (FH) data rate on the feeder link between a non-terrestrial platform and the ground-station for Uplink (UL) communication. The derived calculations are exemplarily evaluated using common system parameters for two typical non-terrestrial communication platforms, the Low Earth Orbit (LEO) satellites and the High Altitude Platform Station (HAPS). In addition to the fulfillment of Timing requirements, computational complexity and on board of flying nodes, the calculated FH data rate will be an important factor for choosing the actual functional split per scenario.**

***Index Terms*—Functional Split (FS), 3D Networks, Non-Terrestrial Communication, 3GPP, Fronthaul Throughput, NTN**

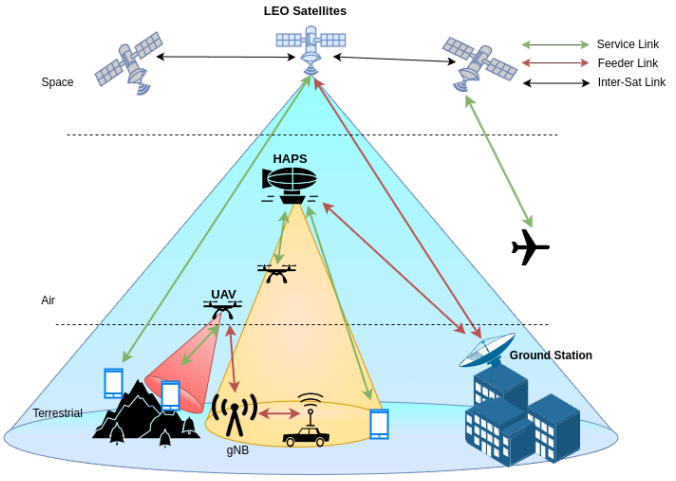

Fig. 1. 3D Network architecture, composed of LEO satellites, HAPS and UAV as a form of HIBS with the different beam size of each non terrestrial node on the ground.

I. Introduction

Current terrestrial networks face limitations in achieving complete coverage due to restricted coverage areas and geographical barriers. Network outages during natural disasters can further disrupt critical operations, jeopardizing lives and property [1]. Three-dimensional (3D) wireless communication networks represent the next frontier in network deployment. These networks leverage a layered approach, integrating space-, air-, and terrestrial-based communication links to achieve seamless and ubiquitous coverage. As we approach the 2030s, the anticipated roll-out of 6G, full integration of non-terrestrial communication links becomes crucial [2]. This includes satellites, mega-constellations in LEO, and airborne platforms such as High Altitude Platform Station (HAPS) and Unmanned Aerial Vehicles (UAVs) as two forms of High Altitude Platforms as IMT base Station (HIBS) working in tandem with TNs. The high number of potential gNodeB (gNB) nodes due to non-terrestrial integration necessitates flexibility, robustness, cost-effectiveness, and energy efficiency in these new platforms. Consequently, integrating the concept of Functional Split (FS) with non-terrestrial platforms becomes a critical step towards achieving these goals.

The 3GPP Release 15 introduced the adaptable design for the 5G Radio Access Network (RAN) [3]. This design disaggregates the traditional gNB into three logical nodes: the Radio Unit (RU), Distributed Unit (DU), and Central Unit (CU). So far, 3GPP has introduced in principle eight FS options for RAN in TNs. In the recent years, the O-RAN alliance, another major player, has focused on physical layer splits and presented its own split based architecture of RAN [4].

Different FS options necessitate varying data rates to transmit the information between nodes as calculated in [5]. These requirements depend on the deployment scenario and the characteristics of the interface between the split components. 3GPP has addressed the calculation of FH data rate for LTE and New

This research was supported in part by the German Federal Ministry of Education and Research (BMBF) within the projects Open6GHub under grant number 16KISK016 and 6G-TakeOff under grant number 16KISK068 as well as the European Space Agency (ESA) under contract number 4000139559/22/UK/AL (AIComS).

Radio (NR) in [6]–[8] in their respective specifications. So far there are detailed studies on FH data rate analysis for each FS option in TNs such as [9], [10]. In case of Non-Terrestrial Network (NTN) scenario, the calculation of needed FH data rate are mainly done by considering the same result of gained for TN like [11]–[13]. Therefore specific constraints in NTN scenario which consider NTN parametrization for FH data rate of each FS option, are not completely investigated.

This paper proposes a general formulation to determine the FH data rate needed for implementing FS in the Uplink (UL) with non-terrestrial platforms in two NTN scenarios.

II. Functional Split for 3D Networks

A. 3D Networks

3D Networks extend conventional TNs by incorporating air- and space-borne network nodes, as shown in Fig. 1. The NTN nodes including air- and space-borne elements like LEO satellites and HIBS provide connectivity between a terrestrial User Equipment (UE) and a ground station connected to the Core Network. Accordingly, we distinguish between two communication links:

1) Service Link: The communication link connecting UE and the non-terrestrial platform, which hosts some part of RAN functionalities.
2) Feeder Link: The communication link between the non-terrestrial platform and the ground station, which hosts the rest of RAN functionalities and is connected to the Core Network.

B. Functional Split in Terrestrial Network

3GPP introduced in principle eight FS options for a gNB, as depicted in Fig. 2, whereas options 4 and 5 are deemed impractical for implementation [4]. O-RAN also has introduced architectures, which decompose network functions into distinct components that can be implemented on various hardware, which have garnered increased attention [14]. O-RAN primarily concentrates on option 7 of the FS proposed by 3GPP, with a focus on separating the RU and DU functions [15]. Depending on specific FSs, there is a trade-off between computational complexity and data rate demand on the fronthaul or midhaul link. Other trade-offs, such as timing requirements, latency restrictions, and link performance, also are of high importance but not in the context of this paper.

C. Functional Split for Non-Terrestrial Network

3GPP has introduced three non-terrestrial access architectures for satellites, including the transparent payload-based, where the satellite acts as a relay between the user and the core [16]; a regenerative payload-based, where the gNB is fully implemented on the satellite [4]; and a regenerative satellite-based gNB-DU, which considers split option 2 with the complete RU and DU implemented onboard the satellite [17]. O-RAN has not yet officially considered its architecture for NTN, while in [18] and [19] O-RAN based NTN has been investigated in term of a possible architecture solution for NTN system.

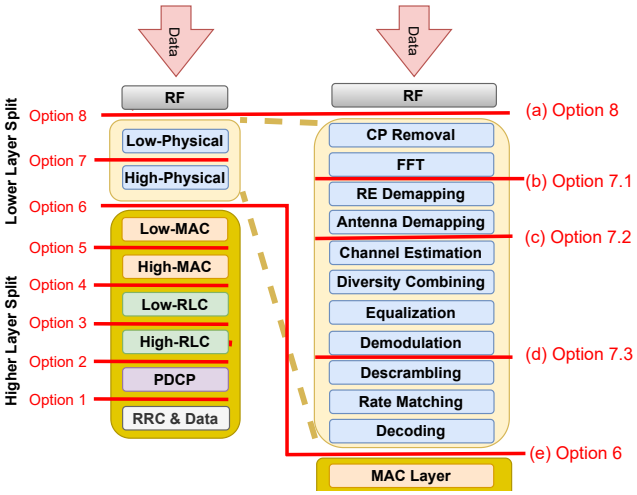

Fig. 2. 3GPP FS in UL. On the left there are eight FS options introduced by 3GPP, and on the right there are lower layer split options in baseband processing unit.

While the 3GPP has currently designated option 2 for NTNs, the push towards a unified 3D network with diverse communication elements necessitates exploring lower layer split options [20], [21] to reduce complexity by not realizing full gNB on the non-terrestrial nodes. For NTN, such lower layer splits lead to a reduced complexity of the NTN nodes as addressed in [13], [22].

The reasons why 3GPP has so far not favored lower layer splits for NTN are mainly timing and latency issues raised for TN as discussed in [16] section 8.4.2. In TN, Downlink (DL) beamforming requires accurate Channel State Information (CSI) gained from the UL channel. In case of lower layer splits, the beamforming is processed in the DU leading to very strict timing requirements between RU and DU. However, in case of LEO satellites it has been demonstrated that beamforming based only on position information of the ground terminals is almost optimal [23]. The beamforming mainly sets the spot on specific position on the Earth surface without requiring current CSI measurements [24]. Thus, the latency requirements for the FH is reduced meaning lower layer split options feasible for UL and DL.

The main challenges regarding lower layer FS for non-terrestrial platforms w.r.t the TN can be listed as:

1) Propagation delay and latency constrains;
2) Level of computational complexity needed onboard, which correlates with energy consumption and cost;
3) High FH data rate over the feeder link;
4) Link reliability and signal quality;

As seen in Fig. 2, split options are classified into high layer and low layer splits. High layer FS reduces the needed FH data rate and more relaxed timing requirements due to reduced dependency on real-time CSI. However, they also raise the complexity and power consumption of the baseband processing. Lower FS, on the other hand, may be advantageous for non-terrestrial nodes since they reduce hardware com-

plexity. The necessity for a balanced approach in the design and implementation of access architectures for non-terrestrial platforms is highlighted by this trade-off. In this paper our baseline for latency, complexity and timing for discussed FS options is based on analysis in [13].

III. System Model

By considering the regenerative access architecture as baseline and prior works of [25]–[27], we focus on the Uplink (UL) case from a UE to the core network through a non-terrestrial node. Fig. 2 shows the block diagram of the baseband processing chain for each FS option from 8 to 6 and their involving functionalities. By moving from FS option 8 towards 6, the FH data rate and latency requirements are reduced, but the computational complexity will increase.

We consider a non-terrestrial communication node operational at the height of h_{C}, so that the number of cells on the ground it can cover is N_{C}. Each cell is served by N_{B} beams and each beam is created by L antenna elements. Therefore, the total number of active antennas is $N_{\mathrm{ant}} = N_{\mathrm{C}} \cdot N_{\mathrm{B}} \cdot L$.

Subsequently, we derived geneal relations for the feeder link data rate per functional split depending on the system parameters. In addition we exemplarity analysis the split options for two common scenarios with parameters specified in Tab. I:

- Scenario 1 (SC1): A LEO satellite at the height $h_{\mathrm{C}} = 600\,\mathrm{km}$ covers $N_{\mathrm{C}} = 19$ cells as outlined in [16],
- Scenario 2 (SC2): A HIBS at the height $h_{\mathrm{C}} = 10\,\mathrm{km}$ covering $N_{\mathrm{C}} = 8$ cells as proposed in [25].

Without loss of generality and for the sake of comparison, we consider based on [3], [16] and [28] that both LEO satellite and the HIBS use the same array and number of antennas, and one beam per cell is considered ($N_{\mathrm{B}} = 1$). Each beam can support a bandwidth of B_{BW}, and the total number of covered UEs in each beam is

$$N_{\mathrm{UE}} = A_{\mathrm{Beam}} \cdot \rho_{\mathrm{UE}} \,. \tag{1}$$

Here, $A_{\mathrm{Beam}} = \pi \cdot r_{\mathrm{Beam}}^2$ denotes the beam foot print size on ground with r_{Beam} is the beam radius as function of platform height, its equivalent antenna aperture and carrier frequency band. Therefore, we have $r_{\mathrm{Beam_{SC1}}}$ equal to $25\,\mathrm{km}$ for S band and $10\,\mathrm{km}$ for Ka band. Furthermore, ρ_{UE} is the UE density per square kilometer $\frac{\mathrm{UEs}}{\mathrm{km^2}}$, which varies depending on the type of communication such as Enhanced Mobile Broadband (eMBB) or massive machine-type communications (mMTC).

The different platform altitudes h_{C} and number of covered users N_{UE} lead to very different Signal to Interference and Noise Ratios (SINRs) allowing for different Modulation and Coding Schemes (MCSs). However, without loss of generality and sake of simplicity the same MCS will be assumed for all covered UEs subsequently.

We assume that each UE has its exclusive access to the entire B_{BW} during its allocated time slot in a Time Division Duplexing (TDD) access, to maximize the data rate during its UL period. Therefore, the non-terrestrial node receives the aggregation of data rates from all UEs across all the time slots. As a result, $N_{\mathrm{UE}} \cdot B_{\mathrm{BW}}$ shows the cumulative data rate demand per each beam over the whole TDD cycle and total service link data rate for whole cells can be written as

$$R_{\text{Service Link}} = N_{\mathrm{C}} \cdot N_{\mathrm{B}} \cdot L \cdot N_{\mathrm{UE}} \cdot B_{\mathrm{BW}} \cdot S \,, \tag{2}$$

in which S is the over sampling rate. All the example parameters are reported with details in Table I. The values are chosen based on different scenarios in the standards [16], [25], [28] from 3GPP.

TABLE I
Example system parameters for FH calculations

Variable Name	Meaning	Value			
N_{C}	No. of covered cells	SC1: 19		SC2: 8	
B_{BW}	Bandwidth (BW) per beam	S band: 30 MHz		Ka band: 400 MHz	
r_{Beam}	Beam radius on the ground	SC1		SC2	
		S:25 km	Ka:10 km	S: 6 km	Ka:6 km
ρ_{UE}	UEs density	eMBB: 0.1 $\frac{\mathrm{UEs}}{\mathrm{km^2}}$		mMTC: 500 $\frac{\mathrm{UEs}}{\mathrm{km^2}}$	
PR	Reference Peak Rate	eMBB		mMTC	
		S: 2 Mbit/s	Ka: 100 Mbit/s	S: 0.256 Mbit/s	Ka:7 Mbit/s
BW_{ref}	Reference bandwidth	S: 5 MHz		Ka: 100 MHz	
N_{B}	No. of beams per cell	1			
L	No.antenna elements create a beam	2			
S	Over sampling rate	1 S/s			
Q_{T}	Quantization in time	16 bits			
Q_{F}	Quantization in frequency	10 bits			
τ_{CP}	CP duration	4.688 µs			
τ_{subframe}	OFDM subframe duration	1 ms			
μ	OFDM numerology	0			
η	Utilization factor	0.6			
N_{S}	No. symbols	14			
N_{SC}	No. of subcarriers	12			
N_{Data}	No. of data REs	110			
M	No. of symbols per beam	2 : 256 QAM			
Q_{LLR}	Quantization per LLR	3 bits			
R_{c}	Code rate	0.64 for $M = 16$			
N_{L}	No. Layer	8			
M_{ref}	Reference modulation order	2 for $M = 2$ and 4, 4 for $M = 16$, 16 for $M = 64$, 64 for $M = 256$			
p_{UL}	Fraction of UEs requesting UL	1 for a fully loaded scenario; 0 for an unloaded system			
S_{UL}	Average content size in UL by UEs	30 B based on [7]			

IV. Fronthaul Rate Calculation for the Functional Split Options

In this section, we utilize the general formulation and variable definitions provided in Section III to derive the calculation of the FH data rates of the considered FS options by 3GPP as shown in Fig. 2. Additionally, we discuss their respective advantages and disadvantages.

A. Option 8: Time Domain

In this FS option, only RF-related processes are performed on the non-terrestrial node. These include analog-to-digital conversion and quantization at each antenna element's output. Assuming perfect sampling, no oversampling occurs, so data volume doesn't increase. Based on [6] upon reception, each sample after analog-to-digital converter is quantized in the time domain using Q_{T} bits per sample per axis (In-Phase and Quadrature), resulting in each sample being represented by $2 \cdot Q_{\mathrm{T}}$ bit. Considering the maximum transmission bandwidth in $R_{\mathrm{ServiceLink}}$ from cells to the non-terrestrial platform we can write

$$R_{\mathrm{Opt8}} = R_{\text{Service Link}} \cdot 2 \cdot Q_{\mathrm{T}} \,. \tag{3}$$

The data to be transmitted over the FH are I/Q samples, which are present even when there is no user data (no load) leading to a constant data rate on the FH link. The primary advantage of option 8 lies in its low onboard complexity leading to reduced

power consumption attributed to minimal signal processing. However, a notable drawback is the very high FH data rate on the feeder link, as the time domain signals are typically represented by $Q_{\mathrm{T}} = 16\,\mathrm{bit}$.

B. Option 7.1: Frequency Domain w/o CP

Option 7.1 involves the removal of symbols designated for OFDM Cyclic Prefix (CP). The CP length is a process dependent variable, represented by the OFDM numerology μ for each subframe. The duration of a single subframe τ_{subframe} for NR is standardized to $1\,\mathrm{ms}$ [4]. The total duration of the CPs per frame is $N_{\mathrm{S}} \cdot (\mu + 1) \cdot \tau_{\mathrm{CP}}$. After the CP removal, the signal is transformed to the frequency domain using the Fast Fourier Transform (FFT). In comparison to the samples in time domain, the samples in frequency domain exhibit a lower dynamic. Thus, the samples can be represented by $Q_{\mathrm{F}} < Q_{\mathrm{T}}$ bits with typically $Q_{\mathrm{F}} = 10\,\mathrm{bit}s$. The rate for this option is

$$R_{\mathrm{Opt7.1}} = R_{\mathrm{Opt8}} \cdot \frac{\tau_{\mathrm{subframe}}}{\tau_{\mathrm{subframe}} + N_{\mathrm{S}} \cdot (\mu + 1) \cdot \tau_{\mathrm{CP}}} \cdot \frac{Q_{\mathrm{F}}}{Q_{\mathrm{T}}} \ . \quad (4)$$

The data rate still is independent of the system load. This FS results in the reduction of data rate by 0.586 for the selected parameters. Option 7.1 does add complexity onboard, however, it is still relatively low, as the required operations are basic and efficient hardware solutions exist.

C. Option 7.2: Resource-Element Demapping

This option follows a procedure outlined in [29], as Resource Element (RE) demapping eliminates blank REs in the received signals according to the system's load, represented by the utilization factor η. After RE demapping, logical antenna ports demapping follows [30] which doesn't change the rate. Thus, the data rate for Option 7.2 can be expressed as

$$R_{\mathrm{Opt7.2}} = R_{\mathrm{Opt7.1}} \cdot \eta \ . \quad (5)$$

The inclusion of REs demapping leads to a reduction in the FH rate, as we now forward only the occupied REs. Therefore, the FH data rate of this option is no more constant and the rate reduction becomes significant in scenarios with very low utilization $\eta \ll 1$. However, the value of η highly depends on the scenario.

D. Option 7.3: Equalization and Demodulation

This option introduces a split in UL motivated by FS option 7.3 for TN of 3GPP. This FS option includes all the functionalities requiring CSI, such as channel estimation, diversity combining, equalization, and demodulation. Therefore, option 7.3 omits the necessity to forward samples for the pilot and reference symbols to the ground station.

Here, the pilots and other reference symbols like Sounding Reference Signals (SRS) and Phase-tracking Reference Signals (PTRS), employed to gain CSI, can be removed, decreasing the FH data rate. Equalization is performed for each beam, which reduces the throughput by a factor of $\frac{1}{L}$ after combining multiple antenna streams into a single beam. After demodulation, there are $\log_2 M$ code bits per symbol, each bit is expressed by Log-Likelyhood Ratio (LLR) with typically $Q_{\mathrm{LLR}} = 3\,\mathrm{bit}$. The resulting FH data rate equals

$$R_{\mathrm{Opt7.3}} = R_{\mathrm{Opt7.2}} \cdot \frac{N_{\mathrm{Data}}}{N_{\mathrm{S}} \cdot N_{\mathrm{SC}}} \cdot \frac{1}{L} \cdot \frac{\log_2 M}{Q_{\mathrm{F}}} \cdot Q_{\mathrm{LLR}} \ . \quad (6)$$

Here, N_{Data} represents all REs dedicated solely for data transmission, whereas $N_{\mathrm{S}} \cdot N_{\mathrm{SC}}$ represents the total number of REs after the CP removal.

By increasing modulation order M, the FH data rate increases as well, as Q_{LLR} bits are forwarded for each code bit. However, novel compression approaches based on the Information Bottleneck Method (IBM) have been designed successfully to limit the information loss by quantization while keeping the relevant information [31]. It is expected, that this technique can significantly reduce the resulting FH rate, while meeting the End-to-End performance constraints [32]. However, the application of IBM-based quantization is beyond the scope of this paper.

The downsides are the considerably increased computation resources.

E. Option 6: Decoding

This option involves several key steps: descrambling, rate dematching, and decoding, which prepare the data for transmission via the feeder link to the ground. Descrambling reorders the data to its original bit order and rate dematching adjusts the data sequence to match the original transmission rate without altering the total number of bits. By the decoding process the information bits are estimated by processing LLR values. Thus, compared to Option 7.3 the data rate is reduced by a $Q_{\mathrm{LLR}}/R_{\mathrm{c}}$ as expressed by

$$R_{\mathrm{Opt6}} = R_{\mathrm{Opt7.3}} \cdot \frac{1}{Q_{\mathrm{LLR}}} \cdot R_{\mathrm{c}} \ . \quad (7)$$

Option 6 offers the advantage of markedly reducing the FH data rate. However, the functionalities involved, particularly the decoding process, entail a considerable degree of computational complexity and energy consumption onboard.

F. Option 2: High-Layer DU/CU split

FS Option 2, proposed by 3GPP as the higher layer split between the CU and DU at the output of Radio Link Control (RLC), particularly for regenerative scenarios, including NTN, and can be considered a baseline. In this option, all signal processing which demands low latency functionality, is performed on the platform (DU side), leading to significantly lower FH requirements and more relaxed latency constraints, but at the cost of increased onboard complexity. The FH data rate on the feeder link can be calculated similar to [7] as

$$R_{\mathrm{Opt2}} = PR \cdot \frac{B_{\mathrm{BW}}}{BW_{\mathrm{ref}}} \cdot \frac{N_{\mathrm{L}}}{N_{L_{\mathrm{ref}}}} \cdot \frac{M}{M_{\mathrm{ref}}} + signaling \quad (8)$$

in which $N_{L_{\mathrm{ref}}} = 1$ as reference number of layer based on [9]. The parameter $signaling = N_{\mathrm{UE}} \cdot p_{\mathrm{UL}} \cdot S_{\mathrm{UL}} \cdot N_{\mathrm{L}}$, is the amount of data as function of load on the system (as p_{UL} shows the percentage of users requesting UL) and the average size of content in UL by users.

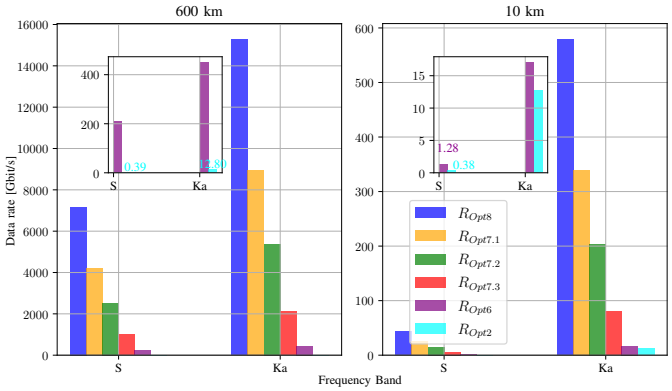

Fig. 3. FH rate for eMBB service with $M = 16$ QAM and $R_c = 0.64$.

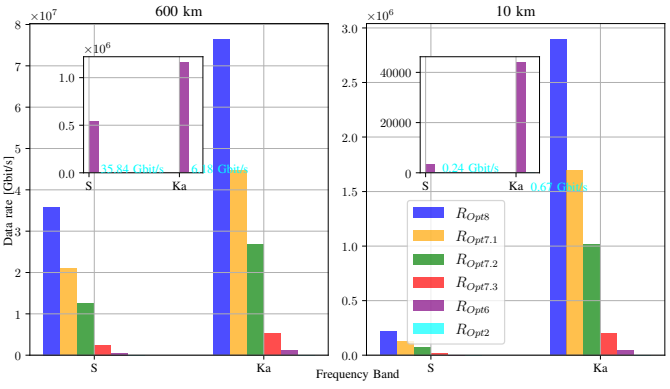

Fig. 4. FH rate for mMTC service with $M = 4$ QAM and $R_c = 0.66$.

V. Results

In this section we present the results of the analysis for the FH data rate of each FS option formulated in Section IV for two described scenarios in Section III. Although that η is different for eMBB w.r.t mMTC but here for sake of comparison we consider η equal for both service the same.

Fig. 3, shows the needed FH data rates for each functional split (FS) option for the two scenarios of LEO satellite at $h_C = 600\,\text{km}$ and HIBS at $h_C = 10\,\text{km}$ for the eMBB service type in case of S and Ka bands, while Fig. 4 shows the same for mMTC service type. The platform altitude, service type, and beam size directly influence the number of users that can be covered. Therefore for SC1:

- in S band
  - $N_{\text{UE}_{\text{eMBB}}} = 3724$
  - $N_{\text{UE}_{\text{mMTC}}} = 18653193$
- in Ka band
  - $N_{\text{UE}_{\text{eMBB}}} = 608$
  - $N_{\text{UE}_{\text{mMTC}}} = 2984520$

And for SC2 since the beam radius is considered equal for both bands:

- $N_{\text{UE}_{\text{eMBB}}} = 88$
- $N_{\text{UE}_{\text{mMTC}}} = 452384$

The needed FH data rate for a higher altitude node like LEO satellite in SC1 is much higher than HIBS in SC2, due to covering more cells and therefore users. For mMTC results in Fig. 4. for both scenarios and B_{BW} the FS options 8 to 6 all show much higher data rate in comparison to eMBB in Fig. 3 due to denser presence of users.

As anticipated, option 8 demands the highest data rate for all cases as time-domain IQ samples for all received signals, independent from the load on the system, are forwarded to ground-station on the feeder link. FS options 7.1, 7.2 and 7.3 reduce the data rate in Fig. 3 in average by 41.3%, 64.8% and 89.7%, respectively, w.r.t option 8 by not adding much more extra complexity on the board. Option 6 can reduce the rate for both frequency bands by 97.9% and 83.34% w.r.t option 8 and 7.3, respectively. The values are closely the same for mMTC service type in Fig. 4. For option 2 as baseline we can see reduction of 99.46% and 97.45% w.r.t option 8 and 7.3, respectively, in cost of adding more functionalities on board. We can conclude that FS option 6 among lower physical layers split demands the least FH data rate and in comparison to option 2 with lower complexity and cost. Depends on the type of service FS option 7.3 can come in the second place, mainly for eMBB.

In case of mMTC service type, option 2 shows the most applicable FH data rate, while option 6 in S band also is feasible.

In Fig. 5, the required FH data rates for FS Options 7.3, 6, and 2 are shown as a function of different modulation orders M and corresponding coding rates R_c for eMBB services, where the HIBS is positioned at $h_C = 10\,\text{km}$. The R_c for each M is selected to maximize spectral efficiency, according to [33]. In case of air-born nodes such as HAPS or UAV, due to their lower altitude and longer visibility in comparison to LEO satellites, the non-terrestrial node based on the request of ground station can ask users to change their MCS based on the received signal SINR to perform link adaptation on the service link. This leads to change in the FH data rate on the feeder link. Option 7.3 increases more by higher modulation order due to the need of sending demodulated bits multiply by the Q_{LLR} factor. Option 6 and 2 show close FH data rate in lower (M, R_c), while after 64 QAM the gap increases, due to the higher code rate. This can be extended as a future work for case of other non-terrestrial nodes such as LEO satellites by performing a link-level simulation.

VI. Conclusion

This paper investigates the FH data rate analysis for FS in the physical layer in case of components of 3D Networks. We have derived the required FH data rate in UL for very general NTN scenario. Based on our results, we have shown that the data rates depend on key parameters, which we can optimized based on the specific requirements of a scenario w.r.t the option 2 CU-DU split as baseline. Our formulation gives the flexibility to extend the analysis for different types of system scenarios as we analyzed two exemplary scenarios

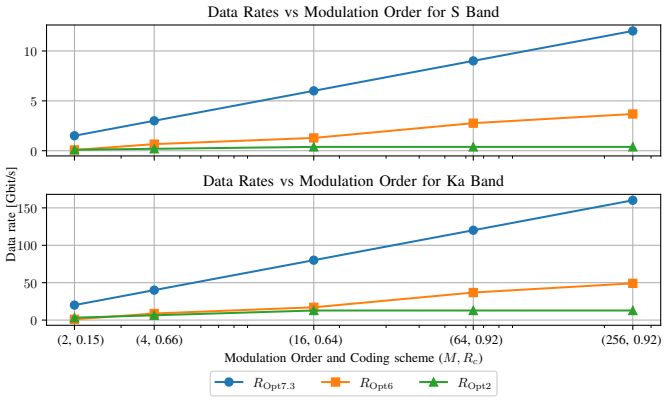

Fig. 5. HIBS needed FH data rate of split options 7.3, 6 and 2 vs modulation order and coding scheme pair for eMBB service.

of LEO and HIBS providing eMBB and mMTC services in frequency bands of S and Ka band. The selection of FS option mainly depends on the use case specifically type of service and frequency band. We can say that FS options 7.2 and 7.3 seems to be good trade-off, while option 6 reduces FH data rate more in cost of complexity increase. While parameters like latency, timing requirements, and energy efficiency are also critical, a thorough analysis of these aspects was beyond the scope of this paper. Future work will extend this study by addressing these additional parameters.

REFERENCES

[1] Y. Wu, S. Singh, T. Taleb, A. Roy, H. S. Dhillon, M. R. Kanagarathinam, and A. De, *6G Mobile Wireless Networks*. Springer, 2021.

[2] G. Geraci, D. López-Pérez, M. Benzaghta, and S. Chatzinotas, "Integrating terrestrial and non-terrestrial networks: 3D opportunities and challenges," *IEEE Communications Magazine*, 2022.

[3] 3GPP, "Study on New Radio (NR) to support non-terrestrial networks (Release 15)," 3GPP, Tech. Rep. TR 38.811 v15.2.0, 2018.

[4] S. Sirotkin, *5G Radio Access Network Architecture: The Dark Side of 5G*. John Wiley & Sons, 2020.

[5] D. Wübben, P. Rost, J. S. Bartelt, M. Lalam, V. Savin, M. Gorgoglione, A. Dekorsy, and G. Fettweis, "Benefits and Impact of Cloud Computing on 5G Signal Processing: Flexible Centralization through Cloud-RAN," *IEEE Signal Processing Magazine*, vol. 31, no. 6, pp. 35–44, Nov 2014.

[6] 3GPP, "CU-DU split: Refinement for Annex A (Transport network and RAN internal functional split)," 3GPP, Tech. Rep. R3-162102, 2016.

[7] ——, "Study on new radio access technology: Radio access architecture and interfaces (Release 14)," 3GPP, Tech. Rep. TR 38.801 v14.0.0, 2017.

[8] ——, "Study on Central Unit (CU) - Distributed Unit (DU) lower layer split for NR (Release 15)," 3GPP, Tech. Rep. TR 38.816 v15.0.0, 2019.

[9] S. Lagén, L. Giupponi, A. Hansson, and X. Gelabert, "Modulation compression in next generation RAN: Air interface and fronthaul tradeoffs," *IEEE Communications Magazine*, 2021.

[10] L. M. Larsen, A. Checko, and H. L. Christiansen, "A survey of the functional splits proposed for 5g mobile crosshaul networks," *IEEE Communications Surveys & Tutorials*, 2018.

[11] S. S. S. G. Seeram, L. Feltrin, M. Ozger, S. Zhang, and C. Cavdar, "Feasibility Study of Function Splits in RAN Architectures with LEO Satellites," *arXiv preprint arXiv:2404.09186*, 2024.

[12] R. Campana, C. Amatetti, and A. Vanelli-Coralli, "RAN Functional Splits in NTN: Architectures and Challenges," *arXiv preprint arXiv:2309.14810*, 2023.

[13] R. Khouli, L. Frank, and A. Hofmann, "Functional split evaluation in NTN for LEO satellites," *IET Conference Proceedings*, 2024.

[14] E. Municio, G. Garcia-Aviles, A. Garcia-Saavedra, and X. Costa-Pérez, "O-RAN: Analysis of Latency-Critical Interfaces and Overview of Time Sensitive Networking Solutions," *IEEE Communications Standards Magazine*, 2023.

[15] E. Sarikaya and E. Onur, "Placement of 5G RAN slices in multi-tier O-RAN 5G networks with flexible functional splits," in *2021 17th International Conference on Network and Service Management (CNSM)*, 2021.

[16] 3GPP, "Solutions for nr to support non-terrestrial networks (ntn) (release 16)," 3GPP, Tech. Rep. TR 38.821 v16.1.0, 2020.

[17] M. Rihan, T. Düe, M. Vakilifard, D. Wübben, and A. Dekorsy, "RAN Functional Split Options for Integrated Terrestrial and Non-Terrestrial 6G Networks," in *2023 11th International Japan-Africa Conference on Electronics, Communications, and Computations (JAC-ECC)*, 2023.

[18] R. Campana, C. Amatetti, and A. Vanelli-Coralli, "O-RAN based Non-Terrestrial Networks: Trends and Challenges," in *2023 Joint European Conference on Networks and Communications & 6G Summit (EuCNC/6G Summit)*, 2023.

[19] F. Matera, M. Settembre, P. Salvo, A. Rago, G. Piro, L. A. Grieco, G. Araniti, S. Pizzi, F. Rinaldi, N. Sambo *et al.*, "From Ground to Space: Towards an Integrated Management of Terrestrial and Non Terrestrial Networks," in *2024 IEEE International Mediterranean Conference on Communications and Networking (MeditCom)*, 2024.

[20] S. Bonafini, C. Sacchi, F. Granelli, S. T. Arzo, M. Devetsikiotis, and K. Kondepu, "HW/SW Development of Cloud-RAN in 3D Networks: Computational and Energy Resources for Splitting Options," in *2023 IEEE Aerospace Conference*, 2023.

[21] R. Bassoli and F. Granelli, "Pico satellites for cloud radio access network," in *2019 IEEE 2nd 5G World Forum (5GWF)*, 2019.

[22] A. Daurembekova and H. D. Schotten, "Unified 3D Networks: Dynamic RAN Functions Placement and Link Challenges," in *ISNCC 2024: International Symposium on Networks, Computers and Communications*, Washington DC, USA, October 2024.

[23] M. Röper, B. Matthiesen, D. Wübben, P. Popovski, and A. Dekorsy, "Position Based Transceiver Design for Multiple Satellite to VSAT Downlink," in *IEEE Open Journal of the Communication Society (OJ-COMS)*, October 2024.

[24] ——, "Beamspace MIMO for satellite swarms," in *2022 IEEE Wireless Communications and Networking Conference (WCNC)*, 2022.

[25] Y. Xing, F. Hsieh, A. Ghosh, and T. S. Rappaport, "High Altitude Platform Stations (HAPS): Architecture and system performance," in *2021 IEEE 93rd Vehicular Technology Conference (VTC2021-Spring)*, 2021.

[26] J. C. Borromeo, K. Kondepu, N. Andriolli, L. Valcarenghi, R. Bassoli, and F. H. Fitzek, "5G NR Support for UAV-Assisted Cellular Communication on Non-Terrestrial Network," in *European Wireless 2022; 27th European Wireless Conference*, 2022.

[27] S. Bonafini, C. Sacchi, R. Bassoli, F. Granelli, K. Kondepu, and F. H. Fitzek, "An Analytical Study on Functional Split in Martian 3-D Networks," *IEEE Transactions on Aerospace and Electronic Systems*, 2022.

[28] S. Euler, X. Lin, E. Tejedor, and E. Obregon, "High-altitude platform stations as international mobile telecommunications base stations: A primer on HIBS," *IEEE Vehicular Technology Magazine*, 2022.

[29] 3GPP, "5G NR Physical channels and modulation," 3rd Generation Partnership Project (3GPP), Technical specification (TS) 38.211, 09 2024, version 18.4.0.

[30] ——, "5G NR; Multiplexing and channel coding," 3rd Generation Partnership Project (3GPP), Technical specification (TS) 38.212, 09 2024, version 18.4.0.

[31] S. Hassanpour, T. Monsees, D. Wübben, and A. Dekorsy, "Forward-Aware Information Bottleneck-Based Vector Quantization for Noisy Channels," *IEEE Transactions on Communications*, vol. 68, no. 12, pp. 7911–7926, Dec 2020.

[32] M. Hummert, S. Hassanpour, D. Wübben, and A. Dekorsy, "Deep Learning-Based Forward-Aware Quantization for Satellite-Aided Communications via Information Bottleneck Method," in *2024 Joint European Conference on Networks and Communications & 6G Summit (EuCNC/6G Summit)*, 2024.

[33] 3GPP, "NR; Physical layer procedures for data," 3rd Generation Partnership Project (3GPP), Technical specification (TS) 38.214, 09 2024, version 18.4.0.